Plant virus evolution under strong drought conditions results in a transition from parasitism to mutualism

Rubén González[a], Anamarija Butković[a], Francisco J. Escaray[b,c], Javier Martínez-Latorre[a], Ízan Melero[a], Enric Pérez-Parets[a], Aurelio Gómez-Cadenas[d], Pedro Carrasco[b], and Santiago F. Elena[a,e,1]

[a]Instituto de Biología Integrativa de Sistemas, Consejo Superior de Investigaciones Científicas - Universitat de València, 46980 Valencia, Spain; [b]Departament de Bioquímica i Biologia Molecular, Universitat de València, 46100 Valencia, Spain; [c]Institut de Biotecnologia i Biomedicina, Universitat de València, 46100 Valencia, Spain; [d]Departament de Ciències Agràries i del Medi Natural, Universitat Jaume I, 12071 Castellón, Spain; and [e]Santa Fe Institute, Santa Fe, NM 87501

Edited by Eugene V. Koonin, National Institutes of Health, Bethesda, MD, and approved December 23, 2020 (received for review October 7, 2020)

Environmental conditions are an important factor driving pathogens' evolution. Here, we explore the effects of drought stress in plant virus evolution. We evolved turnip mosaic potyvirus in well-watered and drought conditions in *Arabidopsis thaliana* accessions that differ in their response to virus infection. Virus adaptation occurred in all accessions independently of watering status. Drought-evolved viruses conferred a significantly higher drought tolerance to infected plants. By contrast, nonsignificant increases in tolerance were observed in plants infected with viruses evolved under standard watering. The magnitude of this effect was dependent on the plant accessions. Differences in tolerance were correlated to alterations in the expression of host genes, some involved in regulation of the circadian clock, as well as in deep changes in the balance of phytohormones regulating defense and growth signaling pathways. Our results show that viruses can promote host survival in situations of abiotic stress, with the magnitude of such benefit being a selectable trait.

virus evolution | mutualism | experimental evolution | gene expression | hormone signaling

Viruses are the most abundant biological entities, having enormous diversity and ubiquitous distribution (1). Traditionally, they have been studied in the context of disease, but nowadays numerous beneficial viruses are being identified in a diverse range of host species (2). Wild plant populations are frequently asymptomatically infected with viruses that in some cases produce diseases in cultivated plants (3). This happens because host–virus interactions fall on a spectrum between pathogenesis and mutualism and during their life cycle viruses might switch between these two lifestyles (4, 5). This transition may happen depending on the environment and the genetics of hosts and viruses (6, 7).

To face frequent environmental abiotic perturbations, plants have evolved acclimatation and tolerance mechanisms. Plant responses triggered by some stressors interact with the response caused by others, e.g., drought and cold (8). This also happens between abiotic and biotic stresses (9, 10), meaning that under certain environmental perturbations (i.e., water availability, extreme temperatures, excess of light irradiation, or oxidative stress) even pathogenic viruses can be beneficial for their host, since infection induces changes in the plant physiological homeostasis that may enhance its survival (7). Drought is one of the main plant stressors that, depending on its intensity and duration, causes major fitness reductions or even death. Xu et al. (11) showed that plants infected with certain viruses can improve their tolerance to drought. It has been shown that the combination of drought and infection with turnip mosaic virus (TuMV) (species *Turnip mosaic potyvirus*, genus *Potyvirus*, family *Potyviridae*) affects different signaling networks in *Arabidopsis thaliana* (L.) Heynh plants (12). Additional examples have been recently summarized in ref. 7. Environmental perturbations can also affect pathogens evolution as changes in the environment can influence the specificity of selection (13).

Here, we have studied how severe drought conditions influence TuMV evolution and, more interestingly, modified the way in which the virus and the host interact at different physiological levels. First, we describe phenotypic and genotypic changes that occur during TuMV evolution under well-watered or dry environments. Second, we characterize the differences in the host's transcriptome and hormonal profiles resulting from the infection with viruses evolved in both conditions. Third, we evaluate the selective pressures on the virus, specifically testing whether evolution under drought conditions selected for viruses that provide an increased tolerance to this adverse environment. The use of diverse natural accessions permitted us to evaluate whether the studied phenomena are plant genotype-specific or general.

Results

TuMV was evolved in four different natural accessions of *A. thaliana* that vary in their responses to infection with potyviruses (14, 15). These accessions classified into two groups according to their phenotypic and transcriptomic responses (15): accessions in group 1 (G1) L*er*-0 and St-0 showed severe symptoms and strong induction of defense genes; accessions in group 2 (G2) Oy-0 and Wt-1 showed milder symptoms and overexpression of genes involved in abiotic stress. An *A. thaliana*-naive TuMV isolate was evolved in each of the accessions for five passages in standard watering or drought conditions.

Significance

Viruses are seen as selfish pathogens that harm their hosts to ensure their own survival. However, metagenomic studies are drawing a new picture in which viruses are present everywhere and not always associated to diseases. A classic observation in plant pathology is that the outcome of infection depends on environmental conditions. Here, using experimental evolution, we show that the relationship between a plant virus and its natural host can evolve from pathogenic to mutualistic under severe drought conditions. While viral strains evolved in normal watering conditions increased their virulence, drought-evolved viral strains confer plants with greater resistance to drought. We show that this transition to mutualism depends on a complex reorganization of hormone-induced signaling pathways and changes in gene expression.

Author contributions: R.G., A.B., A.G.-C., P.C., and S.F.E. designed research; R.G., A.B., F.J.E., J.M.-L., Í.M., and E.P.-P. performed research; F.J.E., A.G.-C., and P.C. contributed new reagents/analytic tools; R.G., A.B., and S.F.E. analyzed data; and R.G., A.B., and S.F.E. wrote the paper.

The authors declare no competing interest.

This article is a PNAS Direct Submission.

[1]To whom correspondence may be addressed. Email: santiago.elena@csic.es.

This article contains supporting information online at https://www.pnas.org/lookup/suppl/doi:10.1073/pnas.2020990118/-/DCSupplemental.

Published February 1, 2021.

Phenotypic and Genotypic Changes in TuMV Lineages Evolved under Standard and Drought Conditions. At the end of the evolution experiment (Fig. 1*A*) we obtained 12 lineages evolved in standard and 10 in drought conditions (2 of the Wt-1 lineages evolved under drought conditions became extinct). All resulting lineages had experienced significant increases in their capacity for infection: Evolved viruses infect more plants and they show symptoms faster. Disease progression has been summarized using the area under the disease progress stairs (*AUDPS*) (16), a value that integrates both infectivity and the speed of inducing symptoms (Fig. 1*B* and Dataset S3). For the viral lineages evolved in G1 accessions, the increase in *AUDPS* was significantly larger when plants were grown in standard than in drought conditions ($P < 0.001$; Fig. 1*B*). Viruses evolved in G2 accessions also showed a significant increase in *AUDPS* relative to the ancestral virus, but this increase was larger for the lineages evolved in plants grown in drought conditions compared to the standard conditions ($P < 0.001$; Fig. 1*B*). When facing abiotic stress, plants adjust their gene expression and metabolism to cope with the stress (17). These physiological changes may facilitate or jeopardize virus adaptation depending on the host genetics.

Next, seeking to characterize the spectrum of mutations in the evolved viral genomes, the nucleotide sequences of the ancestral and evolved viruses were obtained (Fig. 1*C* and Dataset S3). Viruses evolved in standard conditions accumulated 32 mutations; 5 were fixed and 27 were polymorphisms. Nonsynonymous substitutions were the most common type, 27 out of 32 mutations. These mutations were not randomly distributed along the viral genome, but mainly concentrated in the *VPg* cistron (15 out of 32). Viruses evolved in drought conditions accumulated 26 mutations; only 1 was fixed and 25 remained polymorphisms. Again, most mutations were nonsynonymous (21) and preferentially

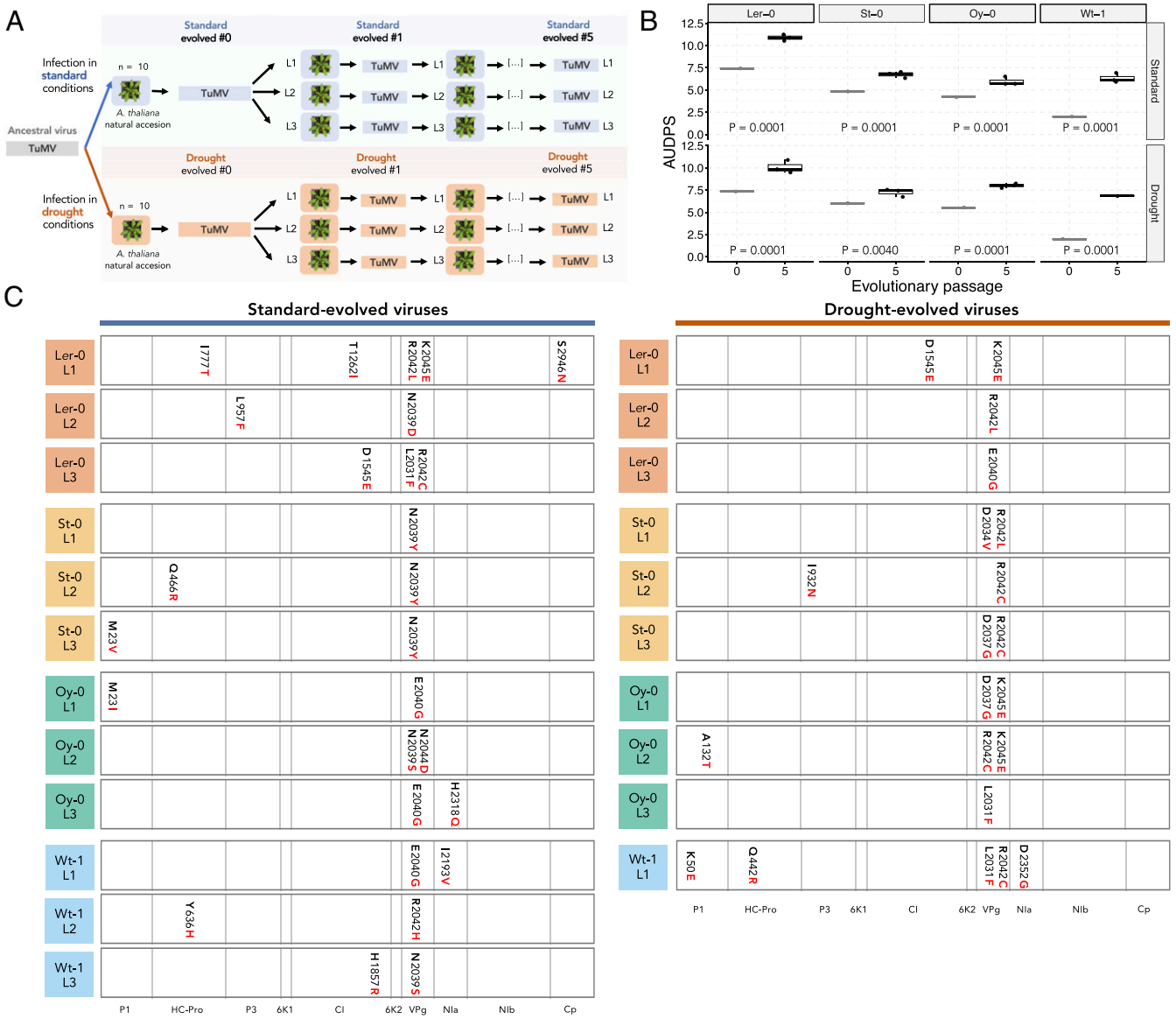

Fig. 1. Experimental evolution of TuMV lineages. (*A*) Experimental design of the evolution experiment. (*B*) *AUDPS* measured at the beginning and after five passages of experimental evolution for viruses evolved in standard (*Upper*) and in drought conditions (*Lower*) for each one of the *A. thaliana* accessions (columns). Significance values from pairwise post hoc Bonferroni tests in the GLM described in Eq. **1**; in all cases, $P \leq 0.004$. (*C*) Mutations found in the standard- (*Left*) and drought-evolved (*Right*) lineages. Each square corresponds with a protein indicated in the lowest row (proportional to the cistron size). Nonsynonymous mutations are indicated with the new amino acid in red.

were observed in the *VPg* cistron. Interestingly, all mutations observed in the *VPg* fall within a narrow domain encompassing amino acids 107–120 (*SI Appendix*, Fig. S1).

As an intrinsically disordered viral protein (18), VPg plays a role in virus–virus and virus–host protein–protein interaction networks (19, 20). It is involved in virus movement, genome replication, and suppression of host antiviral RNA silencing (21, 22). The functional effects of the mutations in the VPg protein were studied in silico using SNAP2 webserver (23) (Dataset S3). Mutations fixed in standard-evolved viruses were predicted to have a significantly weaker effect (mean ± 1 SD = −0.400 ± 22.831) than those fixed in drought-evolved viruses (22.067 ± 26.797) [two-sample *t* test: $t = 6.109$, 28 d.f., $P = 0.020$], which are predicted to be more structurally and functionally disruptive.

Changes in Host's Transcriptomes when Facing Drought and Virus Infection. The whole-genome transcriptomic profiles of plants grown in drought conditions and infected with the drought-evolved viruses were compared with the transcriptomes of plants kept in standard conditions and infected with the standard-evolved viruses. Overall, the number of differentially expressed genes (DEGs) (Dataset S3) was significantly lower in the G1 than in the G2 accessions (Fig. 2*A*; $\chi^2 = 39.953$, 3 d.f., $P < 0.001$).

The functional profiling of the DEGs (Dataset S1) shows a significant overrepresentation of genes involved in circadian rhythm in the underexpressed DEGs of the G1 accessions. All accessions share a few overexpressed or underexpressed genes with other accessions (Fig. 2*B*), some of those few shared genes also showing association with circadian biological events. L*er*-0, Oy-0, and St-0 have in common the underexpression of *PSEUDO-RESPONSE REGULATOR 5* (*PRR5*). The PRR5 protein is a transcriptional repressor of the MYB-related transcription factors involved in circadian rhythm *CIRCADIAN CLOCK ASSOCIATED 1* (*CCA1*) and *LATE ELONGATED HYPOCOTYL 1* (*LHY1*). The repression of *PRR5* would lead to higher levels of *LHY1* expression, a gene that promotes expression of abscisic acid (ABA)-responsive genes responsible for increased tolerance to drought (24, 25). *FLAVIN-BINDING KELCH REPEAT F BOX 1* (*KFK1*), another gene involved in circadian rhythm, is underexpressed in L*er*-0, St-0, and Wt-1. FKF1 stabilizes *CONSTANS* (*CO*) expression and a reduction in *FKF1* expression will result in lower *CO* activity. A *CO*-like gene in rice has been shown to reduce drought resistance when overexpressed and to increase drought tolerance when knocked out (26). These observations align with evidence supporting circadian clock as a contributor to plants tolerance to abiotic stresses (27). Circadian rhythms also play a role in infection, as they affect traits that could increase the fitness of both hosts and parasites (28).

Focusing on biological functions, no significant functional enrichment has been observed for G1 accessions, but for both accessions there is a reduction in DEGs involved in nucleocytoplasmic transport. It has been described that the disruption of genes involved in nuclear transport leads to an increase in drought tolerance (29). In the case of G2 accessions, the number of enriched and depleted biological categories were higher than in the G1 accessions. However, no obvious similarities in the pattern of enrichment between the two G2 accessions were observed. Interestingly, Wt-1 shows an enrichment in defense responses to virus infection, which may explain why two lineages evolved in this accession went extinct early on in the evolution experiment.

To further evaluate how each accession responded to virus infection and drought, the expression of a set of key genes in stress regulation (Fig. 3*A*) were quantified in the combination of all environmental and virus evolution conditions (Dataset S3). Comparison of the gene expression in plants infected with standard- and drought-evolved viruses showed that most of the differential expression happens in the drought environment. Even in these stressful conditions, the number of genes differentially expressed depends on the plant accession that the viruses were evolved in (Fig. 3*B*). With viruses evolved in Oy-0 showing the most extreme differences, especially down-expressing markers are involved in ABA-independent responses (Fig. 3*B*).

These observations suggest that virus adaptation under drought conditions results in a differential change in the local host's transcriptome. Previous work has shown how the degree of adaptation of a potyvirus differentially affects the transcriptome of infected plants (30). It also likely that drought- and standard-adapted viruses alter gene expression by manipulating certain methylation patterns in their host, as recently observed in TuMV lineages naive and well adapted to *A. thaliana* (31), although this hypothesis remains to be tested here.

Differences in Hormone Profiles. Plant response to stresses depends on the fine-tuning among different phytohormones. We have studied the hormonal levels of plants in both environmental conditions, paying attention to differences among noninoculated plants and plants infected with the drought- and standard-evolved viruses (Fig. 4). In both standard and drought conditions, the levels of salicylic acid (SA) were significantly higher in infected plants (regardless in which conditions the virus was evolved) than in noninfected plants (Fig. 4*A*). This increase is expected as SA is a key component in defense signaling, inducing the expression of many defense-related genes (32). However, SA not only plays a role in plant defense but also in plant growth regulation and responses to abiotic stresses (33). Xu et al. found high SA concentrations in plants infected with brome mosaic virus (BMV) and cucumber mosaic virus (CMV), although it could not be unambiguously associated with the improved drought tolerance provided by the infection (11). Aguilar et al. (34) using SA-deficient transgenic lines observed that SA has a role in the tolerance provided by the virus infection. The observed increase in SA levels in infected plants was similar in plants infected with viruses evolved in standard or drought conditions (Fig. 4*A*). Therefore, the enhanced tolerance caused by drought-evolved viruses cannot be solely explained by SA levels, suggesting that other hormones could be also involved. Therefore, ABA, phaseic acid (PA), jasmonic acid (JA), jasmonoyl isoleucine (JA-Ile), oxo-phytodienoic acid (OPDA), and indole-3 acetic acid (IAA) (the main auxin) levels were also quantified (Dataset S3). In standard growth conditions, the only significant difference in the hormonal levels between plants infected with standard- and drought-evolved viruses was for the L*er*-0 accession, where the level of PA is significantly higher in plants infected with standard evolved-viruses (Fig. 4*A*). In drought conditions, the differences are significant for viruses evolved in St-0, with plants infected with the standard-evolved viruses having higher levels of ABA and PA than drought-evolved ones (Fig. 4*A*). Viruses evolved under drought in Oy-0 showed a depletion in ABA and OPDA compared to viruses evolved in standard conditions (Fig. 4*A*).

A principal-component analysis (Fig. 4*B*) shows that the hormonal profile of the four accessions changes in response to the infection status and the growing conditions. Interestingly, ABA shows an expression profile in noninfected plants grown in standard conditions (over the abscissa of the upper left quadrant) that markedly differs from the pattern shown in noninfected plants grown in drought conditions, which actually is similar to the pattern shown by all infected plants, regardless the virus type (in all cases lying in the upper right quadrant). SA clearly distinguishes between infected plants grown in standard (upper right) and drought conditions (upper left) (Fig. 4*B*). JA and JA-Ile also show a highly correlated pattern; while the vectors lie close to the abscissa of the upper right quadrant in noninfected plants grown in standard conditions, they both move to the upper left quadrant in plants infected with drought-evolved viruses kept in standard conditions and move to the lower right quadrant in all other situations (Fig. 4*B*).

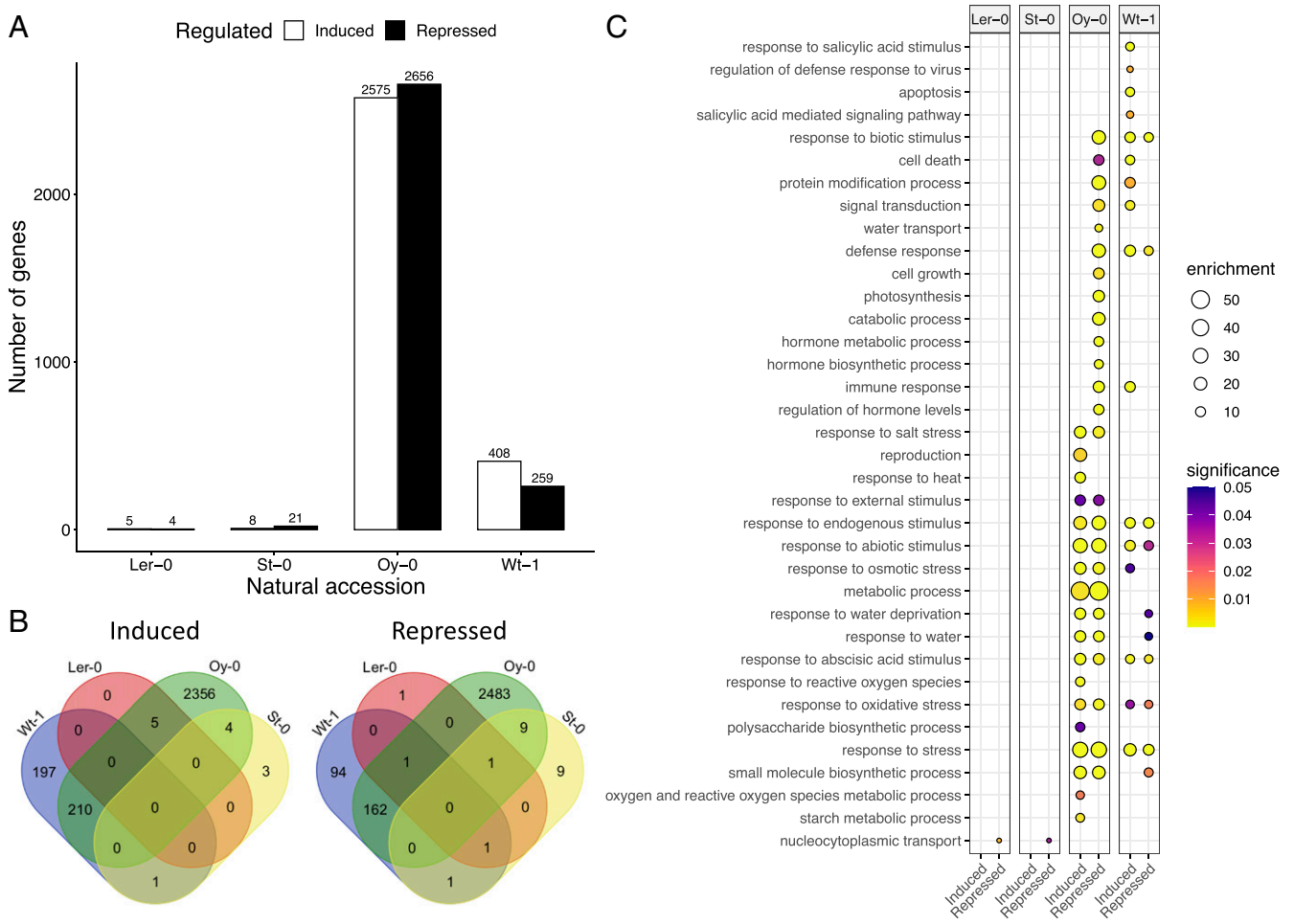

Fig. 2. Transcriptomic responses of different *A. thaliana* accessions to TuMV infection. In each accession, the response of a pool of 8 to 10 plants infected with each one of the corresponding drought-evolved TuMV lineages was compared to the response of plants infected with the standard-evolved viral lineages. (*A*) Number of DEGs obtained for each accession. Overexpressed genes are represented by white bars, and underexpressed genes by black bars. (*B*) Overexpressed (*Left*) or underexpressed (*Right*) DEGs shared between different accessions. (*C*) Gene ontology analysis for DEGs between drought-evolved viruses and standard-evolved ones for each one of the accessions (columns). Circle size represents the level of enrichment, and color indicates adjusted *P* values.

Changes in the Nature of Host–Virus Interactions. We studied the survival of each accession to drought conditions when noninfected or when infected with standard- or drought-evolved viruses (Fig. 5*A* and Dataset S3). L*er*-0 showed almost no survival regardless of its infection status, with no significant differences in mean probability of survival between noninfected plants and plants infected with the standard-evolved viruses ($P = 1.000$) or plants infected with the drought-evolved viral lineages ($P = 1.000$). For the rest of the accessions, plants infected with the standard-evolved viruses had a higher mean survival probability in drought than noninfected plants, although the differences were not statistically significant (Fig. 5*A*; $P \geq 0.202$ in all cases). In sharp contrast, the comparison of mean drought survival probabilities of plants infected with drought-evolved viruses, showed that drought tolerance was significantly higher than in noninfected plants (Fig. 5*A*; $P \leq 0.023$ in all cases). Hence, we conclude that viruses can adapt to promote host tolerance to the environmental perturbations. This may lead to a transition into a mutualistic relationship between the virus and the host as both of them benefit from the infection: The virus is able to replicate and spread while the infected host acquires a physiological and/or morphological change that promotes its survival in the adverse environment (35).

To analyze the specificity of adaptation of each evolved TuMV lineage, we inoculated the 22 evolved viruses into each one of the four accessions and their performance was evaluated using *AUDPS*. With these data, we built up two infection matrices (Fig. 5*B* and Dataset S3), one for plants inoculated with standard-evolved and another with drought-evolved viruses. In each matrix, black squares represent host–virus combinations in which *AUDPS* was equal or greater than the value observed for the viral lineage in its corresponding local host. Therefore, the upper rows correspond to more generalist lineages while the lower ones correspond to more specialist ones. In general, viruses evolved in accessions from G1 (L*er*-0 and St-0) are more generalist than viruses evolved in accessions from G2 (Oy-0 and Wt-1 lineages). Likewise, plants from G2 are more susceptible to infection than those from G1. This indicates that accessions which are more permissive to infection gave rise to less pathogenic viruses regardless of the watering status, while the more restrictive accessions selected for viruses with greater pathogenicity. Similar results have been previously reported for potyvirus–*A. thaliana* pathosystems (36, 37).

Next, we sought to explore whether environmental stress would affect the specificity of adaptation. To quantify the degree of specialization, we calculated the partner diversity d' index

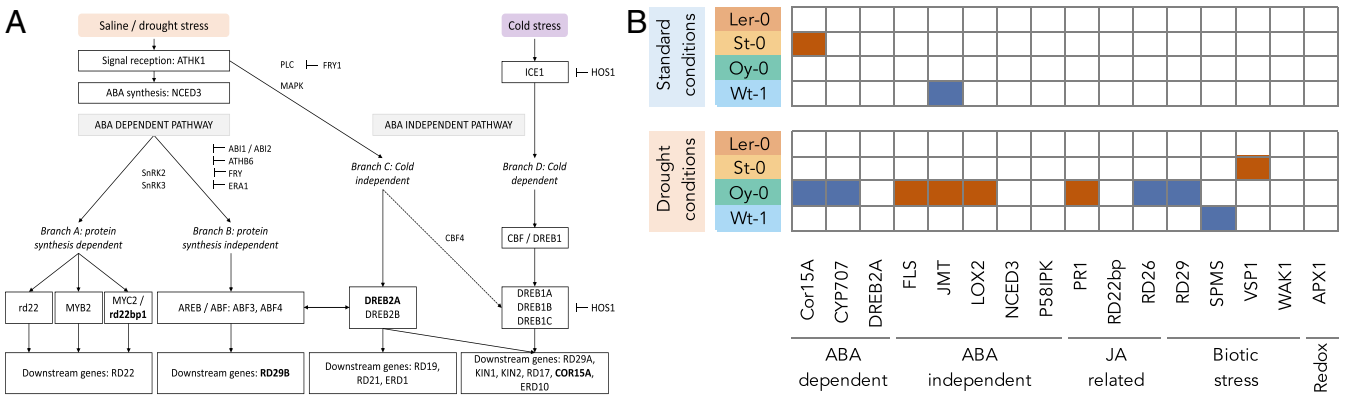

Fig. 3. (*A*) Schematic representation of *A. thaliana* network regulating the response to drought stress; in bold are some of the genes whose expression was evaluated. (*B*) Comparison of the $2^{-\Delta\Delta C_T}$ values of plants infected with standard- or drought-evolved viruses. Significant differences are marked in blue when the levels are significantly higher in plants infected with standard-evolved viruses and in orange when infected by drought-evolved viruses (pairwise post hoc Bonferroni tests in the GLM model described in Eq. **2**; in all cases, $P \leq 0.040$). The accessions and the conditions where the sample was taken from are indicated in the *Left*. Participation of the measured genes in particular responses to stress are indicated under the table.

(38). For the infection matrix estimated for standard-evolved viruses, the value was 372-fold higher ($d' = 0.037$) than in the matrix estimated for drought-evolved viruses ($d' = 0.0001$). This large difference indicates that a severe environmental stress favored the evolution of more generalist viruses that provide higher tolerance to drought to a diverse array of host accessions.

Finally, we evaluated the nestedness and modularity of the two matrices. The infection matrix estimated for the standard-evolved viruses shows a significant *T*-nestedness (39) (Fig. 5 *B*, *Left*; $T = 30.441$, $P = 0.029$), while the matrix estimated for the drought-evolved viruses did not show significant nestedness (Fig. 5 *B*, *Right*; $T = 18.506$, $P = 0.053$). This suggests that virus evolution in standard conditions selects for a gene-for-gene interaction mechanism in which more susceptible hosts select for more specialized viruses while more resistant hosts select for more generalist viruses. However, under drought conditions, this highly specific mechanism has been overcome, suggesting that it may limit the potential advantage provided by the infection. We also studied the modularity of the infection matrices, as the presence of modules suggests that common selective constraints are imposed by different hosts (e.g., G1 and G2) and similar evolutionary solutions are found by viruses. Both matrices show significant *Q*-modularity (40) ($P = 0.019$ for standard-evolved viruses and $P < 0.001$ for the drought-evolved ones), an observation compatible with groups G1 and G2 imposing similar selective constraints. However, the modularity of the matrix obtained for the standard-evolved viruses is 1.735 times larger than for the drought-evolved ones. This approximately twofold reduction in modularity suggests that the selective pressure created by drought conditions is stronger than the selective constrains due to differences among groups of accessions.

Next, we inoculated all of the viral lineages in their corresponding local accessions in both standard and drought conditions. We found no changes in the viral load of both viruses in all accessions (Fig. 6*A*). Despite not being able to observe significant differences in the virus accumulation, viruses evolved in Wt-1 have a lower viral load that results in a significant reduction of *AUDPS* (Fig. 6*B*). The drought-evolved viruses performed worse in Wt-1 accessions than the standard-evolved viruses, an observation that contributes to a better understanding of why two lineages of Wt-1 drought-evolved viruses ended up extinct early in the evolution experiment. Previously, Aguilar et al. (34) observed that the drought tolerance induced by potato virus X and plum pox virus in *Nicotiana benthamiana* and *A. thaliana* was caused by the overexpression of a virulence factor. In contrast, our results suggest that the enhanced host drought tolerance triggered by drought-evolved viruses does not depend on higher virulence.

Discussion

The environment where a virus evolves shapes the virus–host interaction. In general, plant viruses can adapt to extreme drought conditions, but in certain host genotypes this process can be harder. In these refractory hosts, viral populations might be driven to extinction or will reach a lower fitness than they would in standard conditions, as observed in the two Wt-1 lineages that were extinct. Nevertheless, in other host genotypes, plant viruses adapted and increased their fitness equally well regardless of the watering conditions. The environment also influences the mechanisms of selection in virus evolution: 1) the evolutionary solution reached by viruses evolved in drought conditions did not match a gene-for-gene interaction mechanism, 2) drought-evolved viruses tend to be less specialized, and 3) the selective constraints imposed by the host are more diverse under drought conditions.

In our experimental conditions, the drought environment selected for TuMV lineages that confer enhanced and not accession-specific drought tolerance. Therefore, under conditions of drought stress, infected plants will better tolerate water deficit, and consequently, virus replication and transmission will be increased. The underlaying mechanism that promotes drought tolerance seems to be specific for each accession. Hosts whose response to infection was similar also had similar responses to drought during the infection, but even within groups, each accession had a particular response. Differences in the host response are likely triggered by adaptative substitutions in the viral VPg protein. This highly multifunctional protein accumulated mutations in all lineages, but mutations found in drought-evolved lineages were predicted to be more functionally disruptive than the ones fixed in lineages evolved in standard conditions.

The fact that viruses evolved in drought promoted a higher rate of plant survival demonstrates how virus–host interactions are dependent on the environment and their natural history. It was observed before that viral infection can confer drought tolerance to their plant host, but this study 1) explores how abiotic stresses shape the evolution of a host–virus interaction and 2) shows that virus-induced tolerance is a selectable trait encoded in the viral genome. In our study, we have observed that the response to virus infection in drought conditions is diverse within the same species, suggesting that the mechanisms used by viruses to induce drought tolerance are not universal and different mechanisms could be activated depending on the virus and the host genotypes. Xu et al. observed that drought tolerance improved with virus

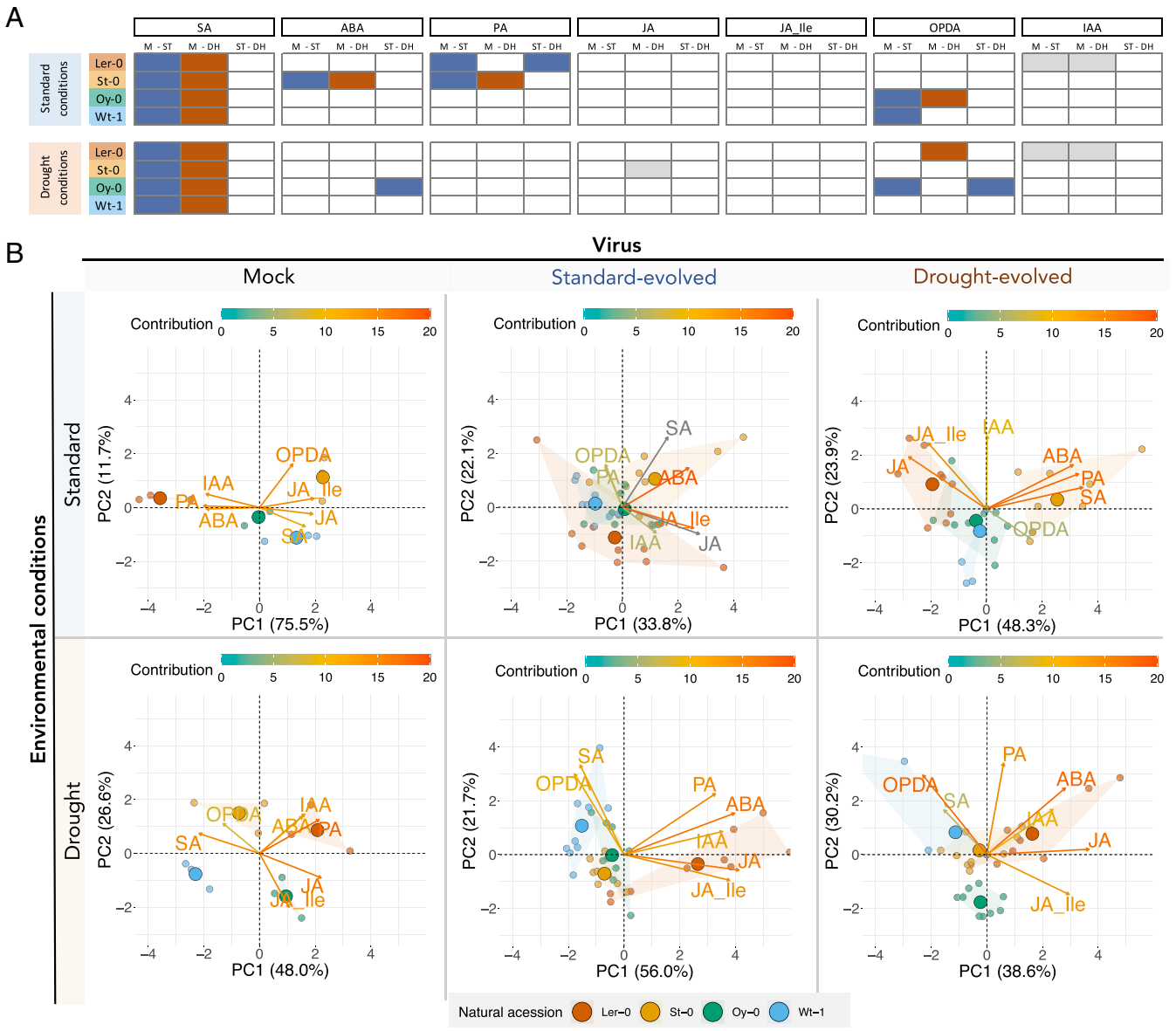

Fig. 4. Quantification of stress-related hormones. (*A*) Comparison of the hormone profiles between noninfected plants (M), plants infected with standard- and drought-evolved viruses. Significant (pairwise post hoc Bonferroni tests the GLM described by Eq. **2**; in all cases, $P \leq 0.039$) differences in the comparation are marked in color: blue when the levels are significantly higher in samples from plants infected with standard-evolved viruses, orange for plants infected with drought-evolved viruses, and gray for noninfected plants. The accessions and the conditions where the sample was taken are indicated in the *Left*. (*B*) Principal-component analysis of the quantified hormones. In all cases, the first two components explain more than 55% of observed variability.

infection and found an increase in several osmoprotectants and antioxidants and that changes in the metabolite profiles were different depending on the pathosystem (11). As an example: trehalose, putrescine, and SA levels were increased in virus-infected plants under water deficit conditions, but proline, ascorbic acid, and sucrose were increased only in BMV-infected rice while galactose, maltose, and anthocyanins were only increased in CMV-infected beet. Aguilar et al. (34) found that hormone levels and metabolite profiles also varied among plants under drought conditions depending on the virus infecting them. Gorovits et al. (41) found that tomato plants infected with tomato yellow leaf curl virus had tolerance to several abiotic stresses. This tolerance was found to be achieved by the viral repression of the ubiquitin 26S proteasome degradation and heat shock transcription factors. The variety in the mechanisms found in different pathosystems parallels the diversity we found within *A. thaliana* accessions.

Bergès et al. (42) illustrated a high level of variability in the response to virus infection and drought within the same species. They studied the response of multiple *A. thaliana* accessions to cauliflower mosaic virus infection in drought conditions. They found that under water-stress symptom appearance and rate of systemic spread is accession dependent. Interestingly, they found that most of the studied accessions had a bigger survival rate during infection when they were cultivated in drought conditions compared to well-watered conditions. The beneficial virus–host interaction under drought conditions may also expand into other organisms that interact with the pathosystem, such as viral vectors. For example, in the pathosystem wheat–barley yellow dwarf virus, it was shown that drought and virus infection enhance the performance of the aphid vector *Rhopalosiphum padi* (43).

As a final take-home message: under environmental perturbations virus–host interactions can evolve, in a relatively short

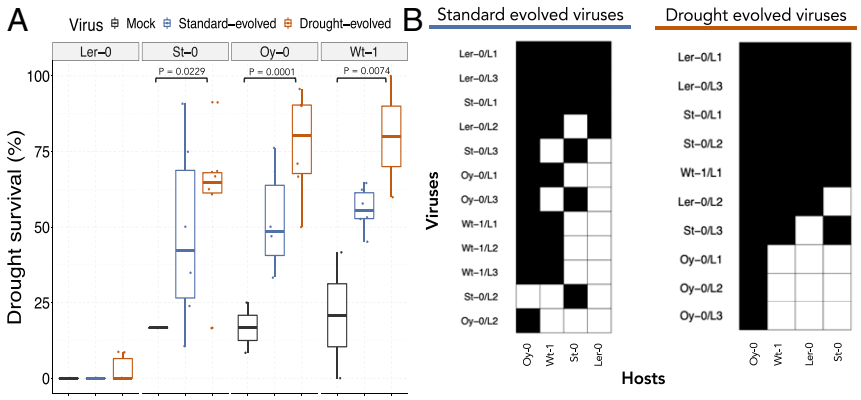

Fig. 5. Host–virus interactions. (*A*) Host survival in severe drought stress in different accessions. Comparison between noninoculated plants (gray), plants inoculated with the standard- (blue) and with the drought-evolved (orange) viruses. Significant differences are marked with brackets, and the *P* values are indicated (pairwise post hoc Bonferroni tests in the GLM described in Eq. **3**). (*B*) Packed infection matrices in standard conditions for standard- and drought-evolved viruses. Viruses used as inocula are ordered (from the most generalist to the most specialist) in the rows and the different hosts (from the most permissive to the least one) in the columns. The black squares represent virus–host combinations in which *AUDPS* was equal or greater than the value observed for the corresponding viral lineage in its corresponding local host.

evolutionary time, from pathogenic to mutualistic. The switch is host genotype dependent, involving alterations in the specificity of virus adaptation along with different host changes underlying regulatory and signaling mechanisms. This shows how viruses can be selected to promote host survival in situations of abiotic stress.

Materials and Methods

Plant Material. Four accessions of *A. thaliana* were used as hosts. These accessions showed different response to potyvirus infection (15) and were classified into two groups according to their response to the potyviral infection: 1) G1, inducing a severe infection, up-regulating defense genes, and shutting down the production of cell wall components (St-0 and L*er*-0), and

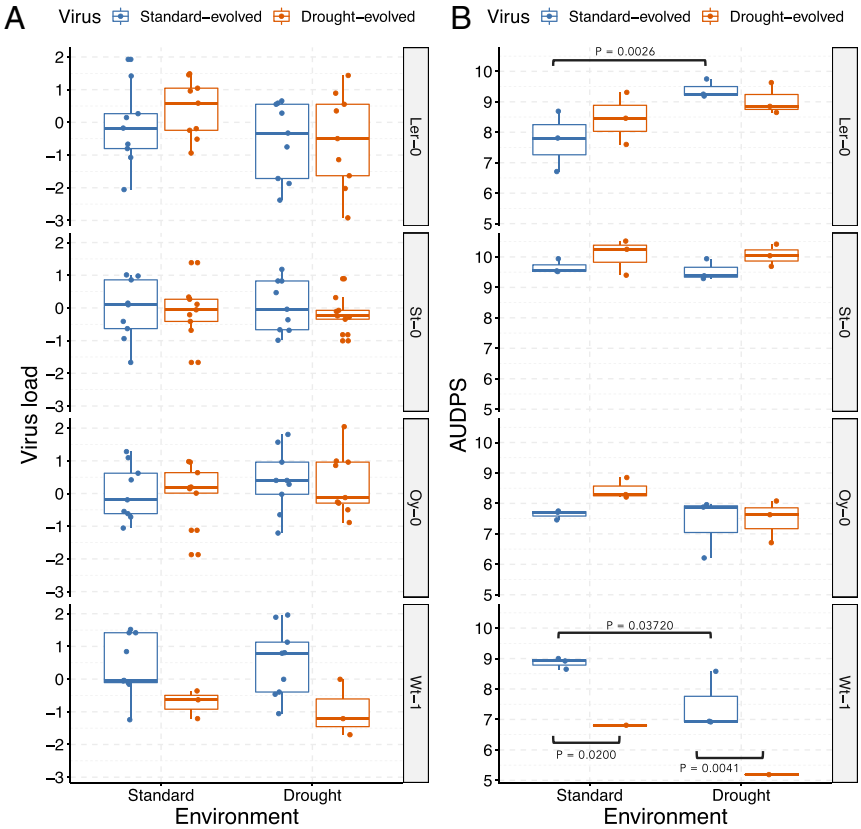

Fig. 6. Two fitness-related traits quantified in standard and drought conditions; blue color for standard- and orange for drought-evolved viruses. Significant differences are marked with brackets, and the *P* values are indicated (pairwise post hoc Bonferroni tests in the GLM described in Eq. **2**). (*A*) *Z* scores of viral loads quantified as copies of *CP* RNA per nanogram of total RNA (the presence of this protein ensures that the whole virus genome was transcribed and no defective particles were quantified). (*B*) Disease progression measured as *AUDPS*.

2) G2, with milder symptoms and lower virus accumulation, up-regulating genes involved in abiotic stress and cell wall construction (Wt-1 and Oy-0).

The selected accessions were exposed to standard watering and drought conditions. Standard conditions consisted of watering every 2 d until the plants were harvested at 14 d postinoculation (dpi). Drought conditions consisted of water withdrawal from 7 dpi until 14 dpi (time at which the plant tissue was harvested).

The evolution experiment was performed in a BSL-2 greenhouse at 24 °C with 16-h light/8-h dark photoperiod. The rest of the experiments were done in a growing chamber at 24 °C with 16-h light/8-h dark photoperiod, 45% relative humidity, and 125 $\mu mol \cdot m^{-2} \cdot s^{-1}$ of light intensity (1:3 mixture of 450-nm blue and 670-nm purple light-emitting diodes).

Experimental Virus Evolution. The infections were initiated using homogenized TuMV-infected tissue preserved at −80 °C. This virus stock was created from infected tissue of *N. benthamiana* plants previously inoculated with an infectious clone derived from TuMV isolate YC5 (GenBank accession no. AF530055.2) from *Zantedeschia* sp. (44).

The stock was used to inoculate four *A. thaliana* accessions. The inoculum used consisted of 100 mg of homogeneous N_2-frozen infected tissue mixed with 1 mL of phosphate buffer and 10% carborundum (100 mg/mL). For each accession, 10 plants were inoculated and kept in standard conditions (well-watered) until infected plants were harvested at 14 dpi and another 10 under drought conditions (no watering from 7 dpi until the harvest at 14 dpi). Only the symptomatic infected plants were collected, making a pool of infected tissue from each condition and accession, using it as inoculum to start a five-passage evolution. For each accession and condition, three lineages were established (Fig. 1*A*).

***AUDPS* Curve.** Upon inoculation, plants were inspected daily for visual symptoms. The infectivity data during the 14 dpi were used to calculate the *AUDPS* as described in ref. 16. This formula transforms data from disease progression, allowing us to express the virulence and dynamics of the disease into a single figure. The *AUDPS* ranges between zero and the total number of observation time points along the experiment; larger *AUDPS* values mean that the virus infects a higher number of plants more quickly. *AUDPS* values were computed using the agricolae R package, version 1.3-2, with R, version 3.6.1, in RStudio, version 1.2.1335.

Depending on the particular experiment being analyzed, *AUDPS* data were fitted to two fully factorial generalized linear model (GLM). In the first type of experiments, plant accession (*A*) and environmental conditions (*C*) were treated as orthogonal factors and evolutionary passage (*t*) as a covariable. The full model equation reads as follows:

$$AUDPS_{ijk}(t) \sim \alpha + A_i + C_j + (A \times C)_{ij} + (A \times t)_i + (C \times t)_j + (A \times C \times t)_{ij} + \varepsilon_{ijk} \quad [1]$$

where α stands for the intercept, and ε_{ijk} represents the Gaussian error associated with each individual *k* plant measured at passage *t*.

In the second type of experiments, plant accession (*A*), environmental conditions being tested (*C*), and environmental conditions where the virus evolved (*E*) were treated as orthogonal factors. The full model equation now reads as follows:

$$AUDPS_{ijkl} \sim \alpha + A_i + C_j + E_k + (A \times C)_{ij} + (A \times E)_{ik} + (C \times E)_{jk} + (A \times C \times E)_{ijk} + \varepsilon_{ijkl}, \quad [2]$$

where α and ε_{ijkl} had the same meaning as in Eq. **1**. In both cases, a Gaussian distribution and identity link function were chosen based on the minimal Bayesian information criterion (BIC) value among competing models. Hereafter, all GLM fitting were done with SPSS, version 26, software (IBM).

In Silico Evaluation of Functional Effects Associated with Observed Mutations in VPg. The functional effects of the mutations in the VPg protein were studied in silico using the Screening for Nonacceptable Polymorphisms (SNAP2) web server (https://rostlab.org/services/snap2web/; last accessed May 20, 2020). SNAP2 machine learning tools provide a score for all possible variants at each residue of the protein (23). This score indicates if there is any effect of the variant in the protein function, regardless if the effect is positive or negative. The score value ranges between −100 (no effect) and 100 (maximal effect).

Next-Generation Sequencing. RNA was extracted from infected plant tissue using Plant RNA Isolation Mini Kit (Agilent). The quality of the RNAs used to prepare RNA-seq libraries was checked with the Qubit RNA BR Assay Kit (Thermo Fisher). SMAT libraries, Illumina sequencing (paired end, 150 bp), and quality check of the mRNA-seq libraries were done by Novogene Europe. Seventeen bases from the 5′ end and 12 from the 3′ of the reads were trimmed with cutadapt, version 2.10 (45). Trimmed sequences were mapped with HiSat2, version 2.1.0 (46), to the ENSEMBL release 47 of the *Arabidopsis* TAIR10 genome assembly. For viral genome SNP calling, trimmed reads were mapped with HiSat2 to the TuMV isolate YC5 with a modified minimum score parameter (*L*, 0.0, −0.8) to allow more mismatches. Resulting SAM files were BAM-converted, sorted, indexed, and analyzed with SAMtools, version 1.10 (47). SNP calling was performed using bcftools, version 1.6, by first using the mpileup subroutine. Read counting in features was done with htseq-count, using The *Arabidopsis* Reference Transcript Dataset (AtRTD2) (48) as input annotation file. Differential expression analysis was done with DESeq2, version 1.24.0 (49), considering only genes having a total of at least 10 reads for each pairwise comparison. Characterization of DEGs was done with plant GOSlim implemented in the Cytoscape plugin Bingo (50) and MapMan (51). Functional profiling was done using gProfiler (52).

RNA Isolation and cDNA Synthesis. Total RNA was extracted from plant tissues using Total Quick RNA Cells and Tissues Kit (Talent SRL), following the protocol established by the manufacturer. Furthermore, DNase treatment (TURBO DNA-free Kit; Ambion) was performed to remove genomic DNA. RNA quantification was performed by spectrophotometric analysis, and its integrity was checked by denaturating agarose gel electrophoresis. The absence of genomic DNA from the RNA samples was additionally tested by the null PCR amplification of the universal rDNA primer pair ITS1/ITS4. Then cDNA was synthetized from 2 μg of total RNA, using SuperScript III H-Reverse Transcriptase (Invitrogen) and 100 pmol of random hexamers (Pharmacia Biotech) according to suppliers' instructions.

Quantitative RT-PCR Analysis. Quantitative real-time PCR (RT-qPCR) was performed on a Thermal Cycler CFX96 Real-Time System (Bio-Rad) using Power SYBR Green PCR Master Mix (Applied Biosystems), 11-μL reactions contained 4.9 μL of 1:6 diluted cDNA samples (8.5 ng of cDNA), 0.3 μL (300 nM) of each primer (forward and reverse), and 5.5 μL of SYBR Green PCR Master Mix. PCR conditions were as follows: two initial steps of 50 °C for 2 min and 95 °C for 2 min, followed by 40 cycles of 95 °C for 30 s and 60 °C for 30 s. Afterward, the dissociation protocol was performed to identify possible unspecific products. Three biological replicates per treatment were analyzed by RT-qPCR. For each transcript, the threshold cycle (C_T) was determined using Bio-Rad CFX Manager 3.1 software. Primers used in the RT-qPCRs are described in Dataset S2.

Viral load was estimated by RT-qPCR using primers that amplify the *CP*. Viral load data were fitted to a fully factorial GLM with the same factors and structure as in Eq. **2**.

Infection Matrices. A full cross-infection experiment was performed where all the 22 evolved lineages were inoculated into 10 plants of all four accessions. Infection matrices were analyzed using tools borrowed from the field of community ecology (53). The statistical properties of the resulting infection matrices were evaluated using the bipartite R package, version 2.11 (54), in R, version 3.6.1 (R Core Team 2016), in RStudio, version 1.2.1335. Three different summary statistics were evaluated: *T*-nestedness (39), *Q*-modularity (40), and overall specialization d' index (38). d' is based in Kullback–Leibler relative entropy, which measures variation within networks and quantifies the degree of specialization of elements within the interaction network. Statistical significance of *T* and *Q* was evaluated using Bascompte et al. (39) null model.

Survival Analysis. Lineages evolved under drought or standard conditions in a certain accession were inoculated in 24 plants of the same accession. Twenty-four plants were mock-inoculated as control. Seven days postinoculation, a severe drought was simulated in the plants by withdrawing water for 14 d. After this period of drought, plants were watered again during 7 d and their survival was evaluated. This experiment was done twice for each one of the four accessions.

Survival frequency (*S*) data were fitted to a factorial GLM in which natural accession (*A*) and type of virus inoculum (*V*) were treated as orthogonal random factors. A binomial distribution and logit link function were chosen based on the minimal BIC value among competing models. The full model equation reads as follows:

$$S_{ijk} \sim \Sigma + A_i + V_j + (A \times V)_{ij} + \varepsilon_{ijk}, \quad [3]$$

where Σ corresponds to the model intercept and ε_{ijk} represents the Gaussian error associated with each individual k plant.

Hormone Quantification. Hormone extraction and analysis were carried out as described in ref. 55 with few modifications. Briefly, plant tissue was extracted in ultrapure water in a MillMix20 (Domel) after spiking with 10 ng of [$^2H_2$]-IAA and 50 ng of the following compounds: [$^2H_6$]-ABA, [C_{13}]-SA, [$^2H_3$]-PA, and dihydrojasmonic acid. Following centrifugation, supernatants were recovered and pH adjusted to 3.0. The water extract was partitioned against diethyl ether and the organic layer recovered and evaporated under vacuum. The residue was resuspended in a 10:90 CH_3OH:H_2O solution by gentle sonication. After filtering, the resulting solution was directly injected into an Acquity SDS ultra-performance LC system (Waters Corporation). Chromatographic separations were carried out on a reversed-phase C18 column (50 × 2.1 mm, 1.8-μm particle size; Macherey-Nagel) using a CH_3OH:H_2O (both supplemented with 0.1% acetic acid) gradient. Hormones were quantified with a TQS triple-quadrupole mass spectrometer (Micromass). Multivariate analysis was perform using the package FactoMineR (56) in R, version 3.6.1 (R Core Team 2016), in RStudio, version 1.2.1335.

Hormones concentration were fitted to a fully factorial GLM with the same factors and structure as in Eq. **2**.

Data Availability. All study data are included in the article and/or supporting information.

ACKNOWLEDGMENTS. We thank Francisca de la Iglesia and Paula Agudo for excellent technical assistance. This work was supported by Grants PID2019-103998GB-I00 and BES-2016-077078 (Agencia Estatal de Investigación–Fondo Europeo de Desarrollo Regional) to S.F.E. and R.G., respectively; GRISOLIAP/2018/005 and PROMETEU2019/012 (Generalitat Valenciana) to S.F.E.; and AICO/2019/150 (Generalitat Valenciana) to A.G.-C. Phytohormone measurements were performed at the Servei Central d'Instrumentació Científica of Universitat Jaume I.

1. D. Paez-Espino *et al*., Uncovering Earth's virome. *Nature* **536**, 425–430 (2016).
2. M. J. Roossinck, The good viruses: Viral mutualistic symbioses. *Nat. Rev. Microbiol.* **9**, 99–108 (2011).
3. M. J. Roossinck, Plant virus metagenomics: Biodiversity and ecology. *Annu. Rev. Genet.* **46**, 359–369 (2012).
4. M. J. Roossinck, Plants, viruses and the environment: Ecology and mutualism. *Virology* **479-480**, 271–277 (2015).
5. M. J. Roossinck, E. R. Bazán, Symbiosis: Viruses as intimate partners. *Annu. Rev. Virol.* **4**, 123–139 (2017).
6. H. R. Prendeville, X. Ye, T. J. Morris, D. Pilson, Virus infections in wild plant populations are both frequent and often unapparent. *Am. J. Bot.* **99**, 1033–1042 (2012).
7. R. González, A. Butković, S. F. Elena, From foes to friends: Viral infections expand the limits of host phenotypic plasticity. *Adv. Virus Res.* **106**, 85–121 (2020).
8. K. Shinozaki, K. Yamaguchi-Shinozaki, M. Seki, Regulatory network of gene expression in the drought and cold stress responses. *Curr. Opin. Plant Biol.* **6**, 410–417 (2003).
9. N. J. Atkinson, P. E. Urwin, The interaction of plant biotic and abiotic stresses: From genes to the field. *J. Exp. Bot.* **63**, 3523–3543 (2012).
10. N. J. Atkinson, C. J. Lilley, P. E. Urwin, Identification of genes involved in the response of *Arabidopsis* to simultaneous biotic and abiotic stresses. *Plant Physiol.* **162**, 2028–2041 (2013).
11. P. Xu *et al*., Virus infection improves drought tolerance. *New Phytol.* **180**, 911–921 (2008).
12. C. M. Prasch, U. Sonnewald, Simultaneous application of heat, drought, and virus to *Arabidopsis* plants reveals significant shifts in signaling networks. *Plant Physiol.* **162**, 1849–1866 (2013).
13. J. Wolinska, K. C. King, Environment can alter selection in host-parasite interactions. *Trends Parasitol.* **25**, 236–244 (2009).
14. J. Lalić, P. Agudelo-Romero, P. Carrasco, S. F. Elena, Adaptation of tobacco etch potyvirus to a susceptible ecotype of *Arabidopsis thaliana* capacitates it for systemic infection of resistant ecotypes. *Philos. Trans. R. Soc. Lond. B Biol. Sci.* **365**, 1997–2007 (2010).
15. J. Hillung, J. M. Cuevas, S. F. Elena, Transcript profiling of different *Arabidopsis thaliana* ecotypes in response to tobacco etch potyvirus infection. *Front. Microbiol.* **3**, 229 (2012).
16. I. Simko, H. P. Piepho, The area under the disease progress stairs: Calculation, advantage, and application. *Phytopathology* **102**, 381–389 (2012).
17. J. Krasensky, C. Jonak, Drought, salt, and temperature stress-induced metabolic rearrangements and regulatory networks. *J. Exp. Bot.* **63**, 1593–1608 (2012).
18. E. Hébrard *et al*., Intrinsic disorder in viral proteins genome-linked: Experimental and predictive analyses. *Virol. J.* **6**, 23 (2009).
19. J. Jiang, J. F. Laliberté, The genome-linked protein VPg of plant viruses—a protein with many partners. *Curr. Opin. Virol.* **1**, 347–354 (2011).
20. F. Martínez *et al*., Interaction network of tobacco etch potyvirus NIa protein with the host proteome during infection. *BMC Genomics* **17**, 87 (2016).
21. F. Revers, J. A. García, Molecular biology of *potyviruses*. *Adv. Virus Res.* **92**, 101–199 (2015).
22. X. Cheng, A. Wang, The *Potyvirus* silencing suppressor protein VPg mediates degradation of SGS3 via ubiquitination and autophagy pathways. *J. Virol.* **91**, e01478-16 (2016).
23. M. Hecht, Y. Bromberg, B. Rost, Better prediction of functional effects for sequence variants. *BMC Genomics* **16** (suppl. 8), S1 (2015).
24. J. H. Westwood *et al*., A viral RNA silencing suppressor interferes with abscisic acid-mediated signaling and induces drought tolerance in *Arabidopsis thaliana*: Virus-induced drought tolerance. *Mol. Plant Pathol.* **14**, 158–170 (2013).
25. S. Adams *et al*., Circadian control of abscisic acid biosynthesis and signalling pathways revealed by genome-wide analysis of LHY binding targets. *New Phytol.* **220**, 893–907 (2018).
26. J. Liu *et al*., Ghd2, a CONSTANS-like gene, confers drought sensitivity through regulation of senescence in rice. *J. Exp. Bot.* **67**, 5785–5798 (2016).
27. J. Grundy, C. Stoker, I. A. Carré, Circadian regulation of abiotic stress tolerance in plants. *Front Plant Sci* **6**, 648 (2015).
28. M. L. Westwood *et al*., The evolutionary ecology of circadian rhythms in infection. *Nat. Ecol. Evol.* **3**, 552–560 (2019).
29. Y. Yang, W. Wang, Z. Chu, J.-K. Zhu, H. Zhang, Roles of nuclear pores and nucleocytoplasmic trafficking in plant stress responses. *Front Plant Sci* **8**, 574 (2017).
30. P. Agudelo-Romero, P. Carbonell, M. A. Pérez-Amador, S. F. Elena, Virus adaptation by manipulation of host's gene expression. *PLoS One* **3**, e2397 (2008).
31. R. L. Corrêa *et al*., Viral fitness determines the magnitude of transcriptomic and epigenomic reprograming of defense responses in plants. *Mol. Biol. Evol.* **37**, 1866–1881 (2020).
32. T. P. Delaney *et al*., A central role of salicylic acid in plant disease resistance. *Science* **266**, 1247–1250 (1994).
33. K. Miura, Y. Tada, Regulation of water, salinity, and cold stress responses by salicylic acid. *Front Plant Sci* **5**, 4 (2014).
34. E. Aguilar *et al*., Virulence determines beneficial trade-offs in the response of virus-infected plants to drought via induction of salicylic acid. *Plant Cell Environ.* **40**, 2909–2930 (2017).
35. J. M. Hily, N. Poulicard, M. Á. Mora, I. Pagán, F. García-Arenal, Environment and host genotype determine the outcome of a plant-virus interaction: From antagonism to mutualism. *New Phytol.* **209**, 812–822 (2016).
36. J. Hillung, J. M. Cuevas, S. Valverde, S. F. Elena, Experimental evolution of an emerging plant virus in host genotypes that differ in their susceptibility to infection. *Evolution* **68**, 2467–2480 (2014).
37. R. González, A. Butković, S. F. Elena, Role of host genetic diversity for susceptibility-to-infection in the evolution of virulence of a plant virus. *Virus Evol.* **5**, vez024 (2019).
38. N. Blüthgen, F. Menzel, N. Blüthgen, Measuring specialization in species interaction networks. *BMC Ecol.* **6**, 9 (2006).
39. J. Bascompte, P. Jordano, C. J. Melián, J. M. Olesen, The nested assembly of plant-animal mutualistic networks. *Proc. Natl. Acad. Sci. U.S.A.* **100**, 9383–9387 (2003).
40. M. E. J. Newman, Modularity and community structure in networks. *Proc. Natl. Acad. Sci. U.S.A.* **103**, 8577–8582 (2006).
41. R. Gorovits, I. Sobol, M. Altaleb, H. Czosnek, G. Anfoka, Taking advantage of a pathogen: Understanding how a virus alleviates plant stress response. *Phytopathol. Res.* **1**, 20 (2019).
42. S. E. Bergès *et al*., Natural variation of *Arabidopsis thaliana* responses to Cauliflower mosaic virus infection upon water deficit. *PLoS Pathog.* **16**, e1008557 (2020).
43. T. S. Davis, N. A. Bosque-Pérez, N. E. Foote, T. Magney, S. D. Eigenbrode, Environmentally dependent host-pathogen and vector-pathogen interactions in the barley yellow dwarf virus pathosystem. *J. Appl. Ecol.* **52**, 1392–1401 (2015).
44. C. C. Chen *et al*., Identification of turnip mosaic virus isolates causing yellow stripe and spot on calla lily. *Plant Dis.* **87**, 901–905 (2003).
45. M. Martin, Cutadapt removes adapter sequences from high-throughput sequencing reads. *EMBnet. J.* **17**, 10 (2011).
46. D. Kim, J. M. Paggi, C. Park, C. Bennett, S. L. Salzberg, Graph-based genome alignment and genotyping with HISAT2 and HISAT-genotype. *Nat. Biotechnol.* **37**, 907–915 (2019).
47. H. Li *et al*.; 1000 Genome Project Data Processing Subgroup, The sequence alignment/map format and SAMtools. *Bioinformatics* **25**, 2078–2079 (2009).
48. R. Zhang *et al*., A high quality *Arabidopsis* transcriptome for accurate transcript-level analysis of alternative splicing. *Nucleic Acids Res.* **45**, 5061–5073 (2017).
49. M. I. Love, W. Huber, S. Anders, Moderated estimation of fold change and dispersion for RNA-seq data with DESeq2. *Genome Biol.* **15**, 550 (2014).
50. S. Maere, K. Heymans, M. Kuiper, BiNGO: A Cytoscape plugin to assess overrepresentation of gene ontology categories in biological networks. *Bioinformatics* **21**, 3448–3449 (2005).
51. O. Thimm *et al*., MAPMAN: A user-driven tool to display genomics data sets onto diagrams of metabolic pathways and other biological processes. *Plant J.* **37**, 914–939 (2004).
52. U. Raudvere *et al*., g:Profiler: A web server for functional enrichment analysis and conversions of gene lists (2019 update). *Nucleic Acids Res.* **47**, W191–W198 (2019).
53. J. S. Weitz *et al*., Phage-bacteria infection networks. *Trends Microbiol.* **21**, 82–91 (2013).
54. C. F. Dormann, B. Gruber, J. Fruend, Introducing the bipartite package: Analyzing ecological networks. *R News* **8**, 8–11 (2008).
55. A. Durgbanshi *et al*., Simultaneous determination of multiple phytohormones in plant extracts by liquid chromatography-electrospray tandem mass spectrometry. *J. Agric. Food Chem.* **53**, 8437–8442 (2005).
56. S. Lê, J. Josse, F. Husson, FactoMineR: An R package for multivariate analysis. *J. Stat. Softw.* **25**, 1–18 (2008).